Vertical Characterization and Transport Dynamics of UTLS Aerosols over Hubei: A Multi-year Integrated Analysis using CALIOP and MERRA-2

Jun Li [1], Jinjing Deng [2], Xin Huang [3], Chuan Zhan [4], Zuohua Miao [5], Qiaozhi Wang [6,*]

[1] College of Resource and Environmental Engineering, Wuhan University of Science and Technology, Wuhan, China – 0108026@wust.edu.cn
[2] Wuhan University of Science and Technology, Wuhan, China – 1164997685@qq.com
[3] Wuhan University of Science and Technology, Wuhan, China – 3336513788@qq.com
[4] Wuhan University of Science and Technology, Wuhan, China – zhanchuan@wust.edu.cn
[5] Wuhan University of Science and Technology, Wuhan, China – ZuohuaMiao@wust.edu.cn
[6] Wuhan University of Science and Technology, Wuhan, China – wangqiaozhi@wust.edu.cn

Keywords: UTLS aerosols, Asian Summer Monsoon, Transport dynamics, CALIOP, Central China.

Abstract:

The upper troposphere and lower stratosphere (UTLS) plays a vital role in the global climate system. Central China, particularly Hubei Province, is located directly downstream of the Tibetan Plateau, making it a key region for observing long-range aerosol transport. In this study, the vertical structure and transport mechanisms of UTLS aerosols over Hubei are investigated using a multi-year (2016-2018) satellite dataset. We applied rigorous Cloud-Aerosol Discrimination (CAD) scores and quality control procedures to nighttime CALIOP profiles to minimize cirrus cloud contamination. Our results show that the UTLS background over this region exhibits low aerosol loading during non-monsoon seasons. However, a substantial aerosol enhancement occurs in summer. The monthly mean extinction coefficient at 14-16 km reaches a peak of 8.05×10^{-3} km^{-1} in August, with a particulate depolarization ratio of ~0.25, indicating the presence of non-spherical particles related to the Asian Tropopause Aerosol Layer (ATAL). To investigate the physical drivers of this seasonal variation, we integrated MERRA-2 meteorological fields and HYSPLIT backward trajectories. The analysis reveals a dual transport mechanism: First, intense local deep convection driven by the East Asian Summer Monsoon (EASM) vertically pumps boundary-layer pollutants into the upper atmosphere. Second, the Asian Summer Monsoon Anticyclone (ASMA) and the westerly jet stream advect aged aerosols horizontally from the Tibetan Plateau to Central China. These findings provide direct observational evidence of how regional monsoon systems synergistically modulate stratospheric aerosol loading.

1. Introduction

The upper troposphere and lower stratosphere (UTLS) crucially regulates the global climate system. Spanning approximately 10 to 20 km above the Earth's surface, this transitional region features a sharp temperature gradient and a complex mixture of chemical species (Yang, 2017). While active weather systems and precipitation typically wash out particulate matter within a few days in the lower planetary boundary layer, the UTLS environment lacks such wet scavenging processes due to its characteristic dryness. Consequently, aerosols injected into this high-altitude layer can survive for months or even years, scattering incoming solar radiation back into space. They also act as essential ice-nucleating particles, directly altering the microphysical properties and formation rates of high-altitude cirrus clouds (Vattioni et al., 2024). Given these strong radiative cooling effects, improving global climate models requires accurate three-dimensional mapping of UTLS aerosols.

However, capturing reliable measurements of UTLS aerosols poses a significant technical challenge. Ground-based lidar networks operate continuously worldwide, but they suffer from severe signal attenuation. The upward-pointing laser beams must travel through the thick, polluted boundary layer and frequently encounter low-altitude clouds, which severely attenuate the optical signal before it reaches the stratosphere. Conversely, passive satellite sensors, such as the Moderate Resolution Imaging Spectroradiometer (MODIS), provide excellent global coverage but integrate the entire atmospheric column into a two-dimensional image, lacking the capability to resolve the vertical altitude of the aerosol layers. Spaceborne active remote sensing provides a direct solution to overcome this vertical blind spot. The CALIOP lidar onboard the CALIPSO satellite emits laser pulses downward from space, bypassing lower-level tropospheric obstructions to deliver highly precise vertical profiles of the UTLS (Winker et al., 2009). Beyond measuring the extinction coefficient, CALIOP records the particulate depolarization ratio, which enables researchers to distinguish non-spherical solid particles (such as lofted dust or crystallized sulfates) from spherical liquid droplets.

Based on these advanced spaceborne lidar observations, atmospheric physicists identified a large-scale recurring seasonal phenomenon: the Asian Tropopause Aerosol Layer (ATAL). During every boreal summer, a highly concentrated aerosol layer forms near the tropopause over the Tibetan Plateau and the Indian subcontinent (Vernier et al., 2015; Vernier et al., 2018). The physical mechanism driving this layer is closely tied to the Asian Summer Monsoon (ASM). The monsoon generates intense surface heating and deep convective thunderstorms, acting as a vertical elevator that transports anthropogenic pollutants and natural dust from the ground into the upper atmosphere. Once these particles reach the UTLS, the Asian Summer Monsoon Anticyclone (ASMA) - a robust closed atmospheric circulation system - traps them. This anticyclone effectively confines the air masses, allowing the pollutants to accumulate and age, thereby creating a stable high-altitude aerosol reservoir (Randel et al., 2010; Fadnavis et al., 2013; Yu et al., 2017). Despite these advances, the downstream transport and vertical structure of ATAL aerosols over densely populated regions east of the Tibetan Plateau remain poorly constrained, motivating the present investigation over Central China.

While the general characteristics of the ATAL over the Tibetan Plateau are well-documented, its downstream expansion and impact on adjacent regions require further investigation. Therefore, we selected the Hubei region in Central China as our primary observational domain. Geographically, Hubei sits in a strategic transitional zone immediately east of the highly elevated Tibetan Plateau and the Sichuan Basin, while connecting to the low-altitude plains of the Yangtze River basin to the east. Although previous studies have mapped the general physical and optical properties of boundary-layer aerosols over Central China (Lu et al., 2018; Fu et al., 2025), the vertical structure and transport dynamics of aerosols specifically within the UTLS over this densely populated region remain largely unexplored. During the summer, the East Asian Summer Monsoon (EASM) heavily influences Hubei with its abundant rainfall and deep convection. Simultaneously, the high-altitude westerly jet stream, forced by the topography of the Tibetan Plateau, flows directly across this longitudinal corridor.

This complex intersection of weather systems raises a critical scientific question: do EASM thunderstorms primarily pump local industrial and urban emissions upward into the summer UTLS over Central China, or does the westerly jet advect them horizontally from the ATAL reservoir over the Tibetan Plateau? To decouple these overlapping transport mechanisms, we processed three full years of nighttime CALIOP profile data (2016-2018) to establish the baseline and capture the summer anomalies of UTLS aerosols. We then integrated MERRA-2 three-dimensional meteorological wind fields and HYSPLIT backward trajectory models to map the exact kinematic pathways of the air masses. By combining high-resolution satellite observations with dynamic meteorological models, this study aims to provide direct evidence of how local monsoon convection and large-scale anticyclonic advection synergistically modulate stratospheric pollution over Central China.

2. Data and Methodology

2.1 Study Area and Geographical Context

The primary observational domain selected for this study is the Hubei region in Central China, spatially defined by the bounding box of 29°N–33°N and 108°E–116°E. The topography of this region makes it a key receptor for long-range aerosol transport. To the immediate west of Hubei lies the Tibetan Plateau, with an average elevation exceeding 4,000 meters, along with the Sichuan Basin. To the east and south, the terrain rapidly descends into the flat, low-altitude plains of the Yangtze River basin, where the elevation drops below 500 meters.

This sharp east-west topographic gradient strongly controls the regional atmospheric dynamics. During the boreal summer, the flat eastern plains allow the East Asian Summer Monsoon to transport large amounts of water vapor inland from the Pacific Ocean. This high moisture content frequently triggers deep convective thunderstorms over Central China. Simultaneously, the prominent orographic barrier of the Tibetan Plateau forces the high-altitude westerly jet stream to accelerate and flow directly across the Hubei corridor. Consequently, this region provides an ideal natural laboratory to observe how local vertical pumping and large-scale horizontal advection interact in the Upper Troposphere and Lower Stratosphere. Figure 1 presents the topographical setting and the spatial coverage of the CALIOP observations used in this study.

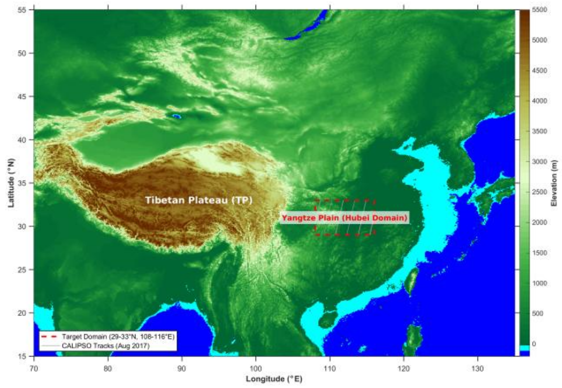

Figure 1. Topographical and geographic overview of the study domain in Central China. The map illustrates the steep elevation gradient (color-shaded relief based on ETOPO dataset) from the highly elevated Tibetan Plateau (TP, deep brown) to the low-lying Yangtze River basin plains (green). The red dashed rectangle (29°N–33°N, 108°E–116°E) explicitly denotes the target study area for data extraction. Superimposed grey solid lines represent the CALIOP ground tracks over the region during the study period (e.g., August 2017), indicating the spatial coverage of the satellite observations.

2.2 CALIOP Lidar Observations and Data Filtering

To obtain the vertical optical properties of aerosols, we utilized the Level 2 Aerosol Profile product (L2 APro, Version 4.20) from the Cloud-Aerosol Lidar with Orthogonal Polarization (CALIOP) instrument onboard the CALIPSO satellite (Winker et al., 2009; Kavosh and Satari, 2026). Our study period covers three consecutive years from 2016 to 2018. The analysis primarily focused on the aerosol extinction coefficient and the particulate depolarization ratio at the 532 nm wavelength. The depolarization ratio serves as a crucial indicator because it helps differentiate non-spherical solid particles (such as dust or crystallized sulfates) from spherical liquid droplets.

Retrieving aerosol signals in the UTLS is subject to high uncertainties due to the low aerosol concentrations and high instrument noise. To mitigate these uncertainties, we implemented a rigorous data screening protocol. First, we discarded all daytime data and only processed the nighttime (ZN) orbital profiles. This step removes the solar background radiation and maximizes the signal-to-noise ratio. Second, the UTLS region frequently contains sub-visual cirrus clouds. These thin ice clouds share similar optical scattering features with coarse aerosols. If the algorithm misclassifies a cirrus cloud as an aerosol layer, it will cause substantial retrieval biases in the extinction calculations. To prevent this, we filtered the dataset using the Cloud-Aerosol Discrimination (CAD) score. We only retained atmospheric bins with CAD scores between -100 and -20. This narrow threshold effectively isolates reliable aerosol signals from ice clouds.

Finally, we applied the Extinction Quality Control (Ext_QC) flags. We only accepted profiles with Ext_QC flags of 0, 1, 16, and 18, which indicate that the lidar ratio was successfully applied without algorithmic divergence. As a result of this stringent filtering, our numerical output frequently showed NaN (Not a Number) values during the winter and spring temporal averaging. We emphasize that these NaN values do not represent missing data; rather, they reflect clean background atmospheric conditions where the actual aerosol concentration falls below the detection limit after removing cloud noise.

2.3 MERRA-2 Assimilated Meteorological Fields

While satellite lidars capture vertical aerosol distributions, they lack concurrent kinematic measurements. To characterize the meteorological background driving the aerosol accumulation, we used the Modern-Era Retrospective analysis for Research and Applications, Version 2 (MERRA-2) (Randles et al., 2017). MERRA-2 provides continuous 3D atmospheric fields by assimilating global observational data.

We downloaded the 3-hourly assimilated meteorological fields (inst3_3d_asm_Nv) at a spatial resolution of $0.5° \times 0.625°$. We specifically extracted the zonal wind velocity (U) and the vertical pressure velocity (ω). We used the U wind to track the horizontal transport speed of the westerly jet stream in the upper atmosphere. In meteorology, ω measures the pressure change of a moving air parcel. Strong negative ω values indicate rapid ascent, serving as a primary dynamical proxy for deep convection. Additionally, we extracted the 3D atmospheric temperature profiles to calculate the thermodynamic tropopause height based on the World Meteorological Organization (WMO) lapse-rate definition. Identifying this dynamic tropopause facilitates the assessment of whether the aerosol layers successfully penetrated into the lower stratosphere.

2.4 HYSPLIT Trajectory Modelling and Source Apportionment

To trace the transport pathways of the polluted air masses arriving over Hubei, we applied the Hybrid Single-Particle Lagrangian Integrated Trajectory (HYSPLIT) model (Stein et al., 2015; Rolph et al., 2017). We drove the trajectory model using the Global Data Assimilation System (GDAS) meteorological fields at a $1° \times 1°$ spatial resolution.

The tracking simulation specifically targeted the most pronounced summer aerosol intrusion events. Based on the CALIOP temporal records, we identified August 5, 2017, as the day with the highest UTLS extinction. We set the HYSPLIT starting locations over the geographic center of Hubei at the core UTLS altitudes of 14 km and 16 km. We ran the model backward in time for 168 hours (7 days). We selected a 7-day tracking window because aerosols in the free troposphere usually reside there for approximately a week prior to broad dispersion. After generating the backward trajectories, we performed a spatial variance clustering analysis to group the air masses into distinct transport pathways. This specific configuration allows us to accurately calculate the percentage contribution of local boundary-layer emissions versus the long-range advection from the Asian Summer Monsoon Anticyclone .

3. Results and Discussion

3.1 The Pristine Background and the Summer Aerosol Intrusion

To establish a robust UTLS aerosol baseline over Central China, we systematically processed an extensive volume of CALIOP Level 2 profile data, encompassing 8,702 orbital files in 2016, 9,207 in 2017, and 9,804 in 2018. Figure 2 illustrates the multi-year monthly mean vertical evolution of the aerosol extinction coefficient and particulate depolarization ratio derived from this large-scale dataset. The temporal distribution reveals a pronounced seasonal contrast. During the non-monsoon months (September to May), the UTLS region (14 – 16 km) remains highly pristine. In the numerical processing, these months frequently yielded NaN (Not a Number) values. As explained in Section 2, these invalid data points resulted from the strict CAD filtering, which effectively eliminated winter cirrus clouds. Consequently, the actual aerosol loading during these periods falls below the fundamental detection limit of the spaceborne lidar.

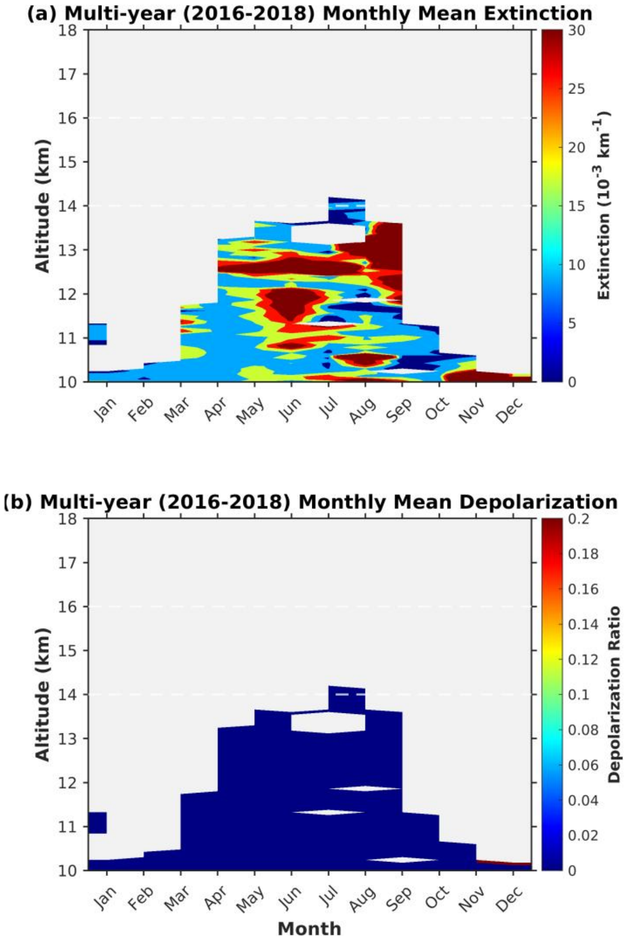

Figure 2. Multi-year (2016-2018) monthly mean evolution of UTLS aerosols over the Hubei region. (a) Extinction coefficient (10^{-3} km^{-1} and (b) Depolarization ratio derived from CALIOP level 2 daily profiles. The horizontal white dashed lines denote the core UTLS altitude band (14–16 km). Areas with invalid or sub-detection-limit data are masked in light gray, highlighting the pronounced seasonal enhancement of fine, spherical aerosols explicitly confined to the boreal summer monsoon period (July–August).

Although sporadic high-extinction events were detected in spring (e.g., May 2018, reaching 31.04×10^{-3} km^{-1} with a depolarization ratio of 0.41, characteristic of typical Asian dust transport), the most persistent and distinct UTLS aerosol enhancement is predominantly concentrated in July and August. Statistical aggregation of the three-year dataset yields 2,082 valid profiles for July and 2,487 for August over the target domain. Analysis indicates that the monthly mean extinction coefficient reaches 7.43×10^{-3} km^{-1} in July and peaks at 8.05×10^{-3} km^{-1} in August. Although this magnitude is relatively small compared to boundary-layer pollution, it constitutes a substantial particulate loading for the typically clean lower stratosphere.

Coinciding with the extinction spike, the satellite recorded elevated particulate depolarization ratios, reaching approximately 0.25 in August. Since spherical particles (e.g., liquid water droplets) generally yield depolarization ratios near zero, a value of 0.25 strongly suggests a high concentration of non-spherical solid particles in the summer UTLS. This specific temporal pattern and optical signature align well with the eastward expansion of the Asian Tropopause Aerosol Layer, as previously documented over the Tibetan Plateau.

3.2 Vertical Pumping by EASM Deep Convection

To elucidate the physical mechanisms driving this summer enhancement, we executed an automated screening procedure across the daily aggregated files to identify extreme UTLS aerosol intrusions. We selected August 5, 2017, which ranked as the most significant summer event (yielding an extinction peak of 8.05 $\times 10^{-3}$ km^{-1} derived from 50 valid profiles), as the primary case study. The meteorological background was then analyzed using MERRA-2 assimilation data. Figure 3 presents the vertical cross-section of the atmospheric dynamics along 31°N, transecting the Hubei region.

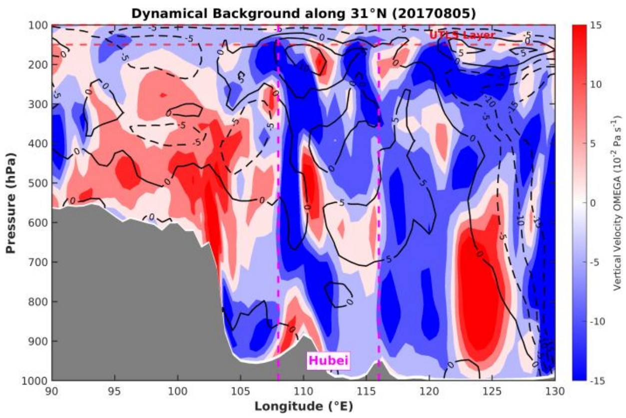

Figure 3. Vertical cross-section of the dynamical background spanning 90°E to 130°E along 31°N during the peak extinction event on August 5, 2017. The color shading indicates the vertical velocity (ω, 10^{-2} Pa s^{-1}, where deep blue regions signify intense upward convection. Solid and dashed black contour lines represent the zonal wind velocity (U, m s^{-1}. The local topography profile is shaded in gray at the bottom. The horizontal red dashed box outlines the focal UTLS layer (150–100 hPa).

The MERRA-2 dynamic fields reveal a typical monsoon-driven deep convective system. Over the target longitudinal corridor (108°E-116°E), the vertical pressure velocity (ω) exhibits a continuous column of strong negative values (dashed contours), indicating intense upward motion. This intense updraft originates in the lower troposphere (~800 hPa) and rapidly penetrates into the UTLS (~150 – 100 hPa). Driven by the East Asian Summer Monsoon, this localized deep convective tower acts as an efficient vertical conduit. It rapidly lofts industrial emissions, carbonaceous aerosols, and moisture directly from the planetary boundary layer into the lower stratosphere. The rapid nature of this vertical transport allows pollutants to largely bypass typical wet scavenging processes in the mid-troposphere.

3.3 Horizontal Advection via the ASMA

While local vertical pumping accounts for the upward flux of boundary-layer particles, it cannot fully explain the mature, widespread aerosol reservoir observed at 15 km. Consequently, we performed a backward trajectory analysis using the HYSPLIT model to trace the long-range transport history. Figure 4 displays the ensemble 168-hour backward trajectories initialized at the core UTLS altitude of 15 km over Hubei on August 5, 2017.

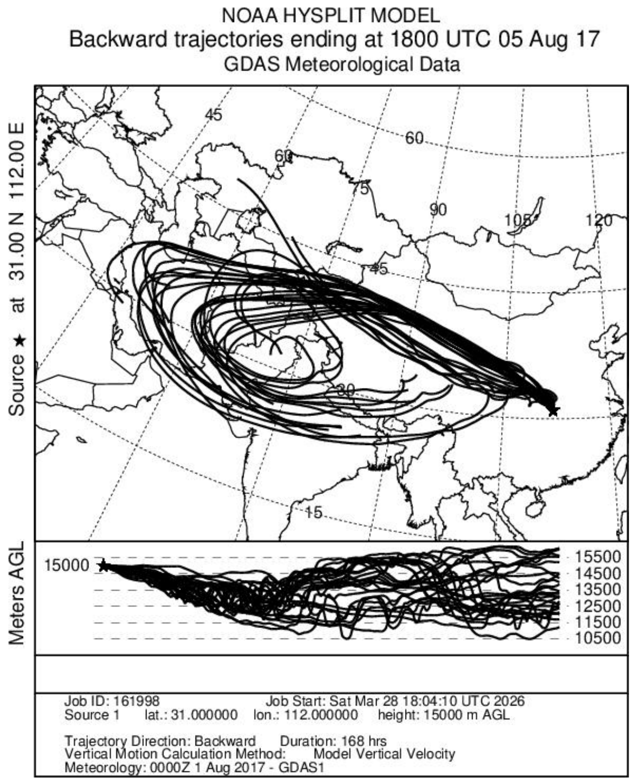

Figure 4. Ensemble 168-hour backward trajectories initialized at an altitude of 15 km over the target region, corresponding to the extreme UTLS aerosol intrusion event on August 5, 2017. The upper panel illustrates the horizontal transport pathways, explicitly capturing the massive anticyclonic circulation pattern characteristic of the ASMA. The lower panel depicts the vertical time-altitude cross-section (meters AGL) of the trajectories, confirming that the advected air masses remained strictly confined within the upper troposphere and lower stratosphere during the long-range transport.

The trajectory mapping reveals a highly consistent horizontal transport pathway. Nearly all simulated trajectory members originated from the west. The air masses trace backward across the Tibetan Plateau, South Asia, and the Middle East, forming a large-scale, closed anticyclonic loop. This specific circulation pattern represents the classic dynamical signature of the Asian Summer Monsoon Anticyclone. Furthermore, the vertical altitude cross-section confirms that these air masses remained strictly confined within the 10.5-15.5 km altitude band over the preceding 7 days. This confinement indicates that the air masses underwent mature, well-mixed stratospheric transport rather than representing a fresh, local boundary-layer injection. The ASMA captures regional emissions from South and Central Asia, ages them within its anticyclonic circulation, and subsequently advects this dense aerosol mixture eastward over Central China via the high-altitude westerly jet stream.

3.4 Synthesis of the Dual-Kinematic Mechanism

Synthesizing the satellite optical measurements, meteorological fields, and trajectory models, we propose a dual-transport mechanism to elucidate the summer UTLS aerosol loading over Central China. As illustrated in the conceptual schematic (Figure 5), the dense aerosol reservoir at 14-16 km results from two interacting dynamical processes. Locally, EASM-driven deep convection provides a strong vertical pumping force, lifting fresh surface pollutants from the eastern plains into the upper atmosphere. Simultaneously, the large-scale ASMA circulation and the westerly jet stream act as a horizontal conveyor belt, advecting aged aerosols from the Tibetan Plateau. The convergence of these two transport pathways over the Hubei geographic corridor well explains the significant extinction peaks and the elevated depolarization ratios observed in the CALIOP records.

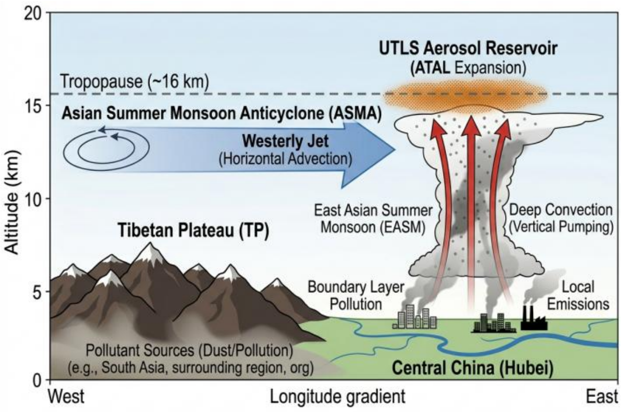

Figure 5. Conceptual schematic illustrating the dual-kinematic mechanism governing the extraordinary UTLS aerosol loading over Central China (Hubei) during the boreal summer. The dense aerosol reservoir (14–16 km) is synergistically fuelled by two distinct dynamical pathways: (1) rapid vertical pumping of boundary layer pollutants driven by East Asian Summer Monsoon (EASM) deep convection (red arrows), and (2) long-range horizontal advection of aged aerosols trapped within the Asian Summer Monsoon Anticyclone (ASMA), transported eastward via the westerly jet stream (blue arrow).

4. Conclusions and future works

In this study, we utilized three years (2016 – 2018) of nighttime CALIOP satellite profiles to characterize the vertical structure of aerosols over the Hubei region in Central China. Our application of rigorous Cloud-Aerosol Discrimination (CAD) filters and quality control flags effectively eliminated sub-visual cirrus clouds and isolated the true aerosol optical properties in the Upper Troposphere and Lower Stratosphere (UTLS). Subsequently, we integrated MERRA-2 three-dimensional meteorological fields and HYSPLIT backward trajectory models to decouple the transport dynamics of these high-altitude aerosols.

Based on this multi-year integrated analysis, our primary conclusions are as follows:

(1) The background UTLS over Central China remains highly pristine from autumn through spring. During these non-monsoon months, the actual aerosol concentrations frequently drop below the fundamental detection limit of spaceborne lidars. However, CALIOP observations capture a substantial and recurring aerosol enhancement during the boreal summer. The monthly mean extinction coefficient in the 14-16 km altitude band peaks at 8.05×10^{-3} km^{-1} in August. The corresponding particulate depolarization ratio reaches approximately 0.25, indicating a high concentration of non-spherical solid particles. This optical signature strongly supports that the Asian Tropopause Aerosol Layer extends significantly eastward over Central China during the summer months.

(2) The integrated analysis reveals that a dual-transport mechanism drives this substantial summer aerosol accumulation. MERRA-2 atmospheric assimilation data demonstrate that localized deep convective systems, driven by the East Asian Summer Monsoon, act as efficient vertical conduits. This strong convection rapidly lifts boundary-layer pollutants from the eastern plains directly into the upper atmosphere. Simultaneously, HYSPLIT ensemble trajectories show that the Asian Summer Monsoon Anticyclone initially traps regional emissions from the Tibetan Plateau and South Asia. The high-altitude westerly jet stream then advects these aged pollutants horizontally over our target region. The convergence of these two transport pathways creates the dense aerosol reservoir over the Hubei corridor.

With their extended atmospheric lifetimes, UTLS aerosols effectively scatter incoming solar radiation and alter the formation of high-altitude clouds (Cuevas et al., 2019; Vattioni et al., 2024). The combination of local vertical pumping and large-scale horizontal advection makes Central China a highly sensitive region to stratospheric pollution. Future studies should incorporate these high-resolution, three-dimensional optical profiles into regional radiative transfer models to quantify the exact climate forcing exerted by the Asian Summer Monsoon. Additionally, relying on a single satellite lidar presents spatial and temporal coverage limitations. Future research should integrate CALIOP observations with other advanced spaceborne lidars (e.g., EarthCARE or CADL) and various passive satellite sensors (e.g., Aura MLS or TROPOMI). Such multi-platform remote sensing synergy will enhance the capability to continuously monitor the long-term kinematic evolution and chemical properties of this UTLS aerosol reservoir.

Acknowledgements

The authors would like to acknowledge the financial support from the WUST Science and Technology Innovation Project for College Students (Grant No. z25059, z26000). We gratefully acknowledge the NOAA Air Resources Laboratory (ARL) for the provision of the HYSPLIT transport and dispersion model and the READY website (https://www.ready.noaa.gov) used in this publication. We also thank the NASA Langley Research Center Atmospheric Science Data Center (ASDC) for providing the CALIPSO/CALIOP Level 2 aerosol data, and the Global Modeling and Assimilation Office (GMAO) at NASA Goddard Space Flight Center for providing the MERRA-2 reanalysis data.

References

Cuevas, E., Romero-Campos, P.M., Kouremeti, N., Kazadzis, S., Räisänen, P., García, R.D., Barreto, A., Guirado-Fuentes, C., Ramos, R., Toledano, C., Almansa, F., Gröbner, J., 2019. Aerosol optical depth comparison between GAW-PFR and AERONET-Cimel radiometers from long-term (2005–2015) 1 min synchronous measurements. *Atmos. Meas. Tech.*, 12, 4309-4337. doi: 10.5194/amt-12-4309-2019

Fadnavis, S., Semeniuk, K., Pozzoli, L., Schultz, M.G., Ghude, S.D., Das, S., Kakatkar, R., 2013. Transport of aerosols into the

UTLS and their impact on the Asian monsoon region as seen in a global model simulation. Atmos. *Chem. Phys.*, 13, 8771-8786. doi: 10.5194/acp-13-8771-2013

Fu, T.Y., He, Y., Jia, Y., Jing, D.Z., Yi, F., 2025. Lidar observations of optical properties of two upper troposphere and lower stratosphere aerosol plumes at Wuhan. *Atmos. Res.*, 327, 108347. doi: 10.1016/j.atmosres.2025.108347

Kavosh, M.T., Satari, M., 2026. Aerosol extinction coefficient estimation over the European troposphere and lower stratosphere using CALIOP profiles. *Atmos. Res*., 328, 108448. doi: 10.1016/j.atmosres.2025.108448

Lu, X., Mao, F.Y., Pan, Z.X., Gong, W., Wang, W., Tian, L.Q., Fang, S.H., 2018. Three-Dimensional Physical and Optical Characteristics of Aerosols over Central China from Long-Term CALIPSO and HYSPLIT Data. *Remote Sens*., 10(2), 314. doi: 10.3390/rs10020314

Randel, W.J., Park, M., Emmons, L., Kinnison, D., Bernath, P., Walker, K.A., Boone, C., Pumphrey, H., 2010. Asian Monsoon Transport of Pollution to the Stratosphere. *Science*, 328(5978), 611-613. doi: 10.1126/science.1182274

Randles, C.A., da Silva, A.M., Buchard, V., Colarco, P.R., Darmenov, A., Govindaraju, R., Smirnov, A., Holben, B., Ferrare, R., Hair, J., Shinozuka, Y., Flynn, C.J., 2017. The MERRA-2 Aerosol Reanalysis, 1980 Onward. Part I: System Description and Data Assimilation Evaluation. *J. Clim.*, 30(17), 6823-6850. doi: 10.1175/JCLI-D-16-0609.1

Rolph, G., Stein, A., Stunder, B., 2017. Real-time Environmental Applications and Display sYstem: READY. *Environ. Model. Softw.*, 95, 210-228. doi: 10.1016/j.envsoft.2017.06.025

Stein, A.F., Draxler, R.R., Rolph, G.D., Stunder, B.J.B., Cohen, M.D., Ngan, F., 2015. NOAA'S HYSPLIT atmospheric transport and dispersion modeling system. *Bull. Amer. Meteor. Soc*., 96, 2059-2077. doi: 10.1175/BAMS-D-14-00110.1

Vattioni, S., Käslin, S.K., Dykema, J.A., Beiping, L., Sukhodolov, T., Sedlacek, J., Keutsch, F.N., Peter, T., Chiodo, G., 2024. Microphysical interactions determine the effectiveness of solar radiation modification via stratospheric solid particle injection. *Geophys. Res. Lett.,* 51(19). doi: 10.1029/2024GL110575

Vernier, J.-P., Fairlie, T.D., Natarajan, M., Wienhold, F.G., Bian, J., Martinsson, B.G., Crumeyrolle, S., Thomason, L.W., Bedka, K.M., 2015. Increase in upper tropospheric and lower stratospheric aerosol levels and its potential connection with Asian pollution. *J. Geophys. Res. Atmos.*, 120, 1608-1619. doi: 10.1002/2014JD022372

Vernier, J.-P., Fairlie, T.D., Deshler, T., Venkat Ratnam, M., Gadhavi, H., Kumar, B.S., Natarajan, M., Pandit, A.K., Akhil Raj, S.T., Hemanth Kumar, A., Jayaraman, A., Singh, A.K., Rastogi, N., Sinha, P.R., Kumar, S., Tiwari, S., et al., 2018. BATAL: The Balloon Measurement Campaigns of the Asian Tropopause Aerosol Layer. *Bull. Amer. Meteor. Soc.*, 99(5), 955-973. doi: 10.1175/BAMS-D-17-0014.1

Winker, D.M., Vaughan, M.A., Omar, A., Hu, Y., Powell, K.A., Liu, Z., Hunt, W.H., Young, S.A., 2009. Overview of the CALIPSO Mission and CALIOP Data Processing Algorithms. *J. Atmos. Ocean. Technol.*, 26(11), 2310-2323. doi: 10.1175/2009JTECHA1281.1

Yang, J.M., 2017. Towards a combined SAGE II and SCIAMACHY aerosol dataset and implications for stratospheric aerosol trend analysis over East Asia. Atmos. *Ocean. Sci. Lett.,* 10(5), 343-347. doi: 10.1080/16742834.2017.1341812

Yu, P., Rosenlof, K.H., Liu, S., Telg, H., Thornberry, T.D., Rollins, A.W., Portmann, R.W., Bai, Z.X., Ray, E.A., Duan, Y.J., Pan, L.L., Toon, O.B., Bian, J.C., Gao, R.S., 2017. Efficient transport of tropospheric aerosol into the stratosphere via the Asian summer monsoon anticyclone. *Proc. Natl. Acad. Sci. U.S.A.*, 114(27), 6972-6977. doi: 10.1073/pnas.1701170114